Dynamic Frequency Planning for Autonomous Mobile 6G in-X Subnetworks

Valentin Thomas Haider*, Rastin Pries†, Wolfgang Kellerer*, and Fidan Mehmeti*
*Chair of Communication Networks, Technical University of Munich, Germany, {firstname.lastname}@tum.de
†Nokia, Munich, Germany, rastin.pries@nokia.com

***Abstract*—Within the development of 6G, so-called subnetworks were proposed to serve special use cases like intra-vehicle sensor-actuator communication, robot control in industrial environments, or health monitoring. These use cases are characterized by extreme communication demands between the devices served by a single subnetwork. Moreover, the subnetworks will be densely deployed, with mobile and autonomous vehicles carrying the subnetwork Access Points (APs). These properties necessitate novel approaches for frequency planning in order to enable reliable communication within all subnetworks and efficient resource usage. In this context, the problem of dynamic frequency planning for mobile 6G in-X subnetworks is investigated in this paper. To this end, a multi-objective optimization problem with the objectives of minimizing frequency subband usage and subnetwork reconfigurations leveraging knowledge about future interference scenarios is formulated. Afterward, the problem is shown to be NP-hard, and two heuristic algorithms are developed. Using realistic vehicular movement data from simulations, results show that the heuristics outperform a State-of-the-Art (SotA) benchmark. Moreover, the value of knowledge about future interference scenarios is shown. Reconfigurations can be reduced by 18.91 % when prioritizing subband usage and even by 33.02 % when prioritizing reconfigurations if interference scenarios are known for three time steps instead of one.**

***Index Terms*—6G, Frequency Planning, Multi-Objective Optimization, Resource Allocation.**

I. Introduction

Since the very first generation of mobile communication networks, frequency planning has been considered an extremely important task in the deployment and management of mobile communication networks [1]–[4]. There exist two main reasons for this: Firstly, in general, the available frequency spectrum for radio communications is scarce [1], which necessitates reusing frequency spectrum to ensure high spectral efficiency [4]. Secondly, reusing spectrum potentially causes interference, which thus requires adequate frequency planning for mitigating or preventing co-channel and adjacent channel interference to enable stable communication links while using the available resources in an effective way [3], [4].

For 6G networks, which are currently under development, so-called subnetworks are envisioned to be deployed within industrial environments, in vehicles, or carried by drones to service users in geographically confined areas like cars, factories, or dense urban areas [5]–[9]. There exist three different operation modes: In the standalone mode, the subnetwork operates autonomously, while in the semi-autonomous or connected mode, the subnetwork can receive control information from the umbrella network, and the subnetwork Access Point (AP) can act as a gateway to the umbrella network [9], [10]. The goal of these subnetworks is to provide high data rates, extremely low latency, reliability, and resilience for use-cases like intra-vehicle sensor-actuator communication [5], [6], robot control in industrial environments [8], [11], or in-body networks for health monitoring [9], [10].

This work was supported by the Federal Ministry of Education and Research of Germany (BMBF) under the projects "6G-Life" and "6G-ANNA", with project identification numbers 16KISK002 and 16KISK107.

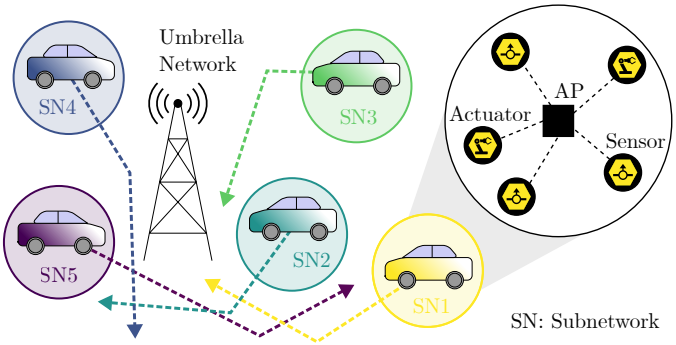

Fig. 1. Illustration of mobile 6G subnetworks and their trajectories with the subnetwork APs deployed in vehicles connecting sensors and actuators.

The main objective of subnetworks is to facilitate communication between User Equipments (UEs) that are all in the vicinity of the same subnetwork AP. Hence, subnetworks are considered substantially different from pico- or femtocells known from traditional cellular networking, which aim to increase coverage and connect the UEs to the internet [7]. Moreover, 6G subnetworks fundamentally differ from relay nodes, which do not use their own spectrum and merely forward messages [12]. While *standalone* 6G subnetworks are similar to private 5G networks which are completely isolated [13], the focus of this work is *semi-autonomous* or *connected* subnetworks. Thus, a new network architecture and purpose are considered. Still, as for all radio communication systems, also 6G subnetworks require frequency bands from either licensed or unlicensed spectrum to offer their services.

Many 6G subnetworks will be mobile due to the deployment of subnetwork APs within autonomous vehicles, Unmanned Aerial Vehicles (UAVs), or robots. An illustration of such a system is depicted in Fig. 1. The mobility of the subnetworks makes the allocation of frequency spectrum to the subnetworks a complicated task. Moreover, these networks are envisioned to be deployed with extremely high densities of several tens of

thousands of subnetworks per km^2 [10]. Nevertheless, the autonomy of the vehicles carrying the subnetworks grants knowledge about their future movement trajectories, which allows predicting possible future interference scenarios between the subnetworks. Hence, the operation of these networks requires more advanced frequency planning methods exploiting this knowledge to efficiently use the available frequency spectrum and to guarantee interference-free operation of all subnetworks within a certain geographical area at all times [7], [11], [14].

Several interesting questions arise related to the frequency planning for mobile 6G subnetworks:

- Firstly, given the mobility trajectories of mobile subnetworks, what is the optimal frequency subband allocation to minimize the overall spectrum consumption and subnetwork reconfigurations while guaranteeing interference-free operation of all subnetworks?
- Secondly, how does the amount of knowledge about future interference scenarios influence the overall frequency resource consumption over time?

To answer these questions, this paper investigates the problem of frequency subband allocation for mobile 6G subnetworks. To this end, a multi-objective optimization problem with the objectives of minimizing spectrum consumption and subnetwork reconfigurations is formulated, which ensures efficient resource usage and minimal signaling overhead. Thereby, the resource demand of every subnetwork provider is modeled in a generic way to facilitate different allocation granularities. Moreover, interference between two subnetworks is classified as a binary input to the optimization, i.e., it is determined whether or not there exists interference at a certain point in time. This input classification allows for employing various methods for interference classification. The optimization problem is then analyzed and proven to be NP-hard. Subsequently, different general solution approaches are discussed and two heuristic algorithms are developed. The different solution methods are ultimately evaluated using simulations. The presented results provide valuable insights for making mobile subnetworks a reality in future 6G communication systems. Specifically, the main contributions are:

- Formulating a multi-objective optimization problem for frequency subband allocation to mobile 6G subnetworks enabling interference-free operation (Section III);
- Proving the NP-hardness of the formulated optimization problem and discussing its solution space (Section IV);
- Developing two heuristic algorithms to solve the optimization problem in polynomial time (Section IV);
- Performing extensive simulations based on realistic vehicle mobility patterns and highlighting the value of knowledge about future interference scenarios (Section V).

II. Related Work

Many works exist on resource management and interference mitigation for 6G in-X subnetworks, mainly focusing on the resources frequency subbands and transmission power. These works can be categorized into centralized and distributed decision-making, whereas the allocation problems are mainly solved using heuristics or Machine Learning (ML).

The works focusing on transmission power selection or allocation aim to optimize different communication quality aspects like maximizing the achieved rates within subnetworks [15], maximizing the overall network's sum spectral efficiency [16], [17], maximizing the control performance of plants based on sensor-actuator communication [18], or minimizing the sum interference-to-signal power ratios across all the subnetworks [19]. The authors of [20] propose postponing message transmissions and transmission power reduction to decrease interference and increase the probability of medium access for subnetworks operating on unlicensed spectrum. While some of these works also guarantee minimum target rates or spectral efficiencies using constraints during the optimization [15], [17], interference-free communication is never targeted, which might be necessary especially for life-critical services [14] or scenarios with highly varying channel conditions.

Similarly to the works regarding power management, the research on frequency (sub-)channel allocation focuses on, e.g., maximizing all subnetworks' sum rates or minimizing the sum interference-to-signal ratio over all subnetwork links. While distributed approaches like [11], [21]–[28] support full autonomy of all subnetwork APs, these approaches cannot guarantee interference-free operation even though some works consider the possibility of selecting multiple (sub-)channels [15], [22], [27]. Most of these works rely on Reinforcement Learning (RL) or other ML approaches to select channels based on, e.g., Received Signal Strength Indicator (RSSI) values or interference power measurements [11], [21]–[24], [26], [28], whereas there exist only few papers relying on heuristic approaches [25], [27]. Centralized subband allocation is solved using a Graph Neural Network (GNN) or a Deep Neural Network (DNN) in [28] or [29], or using a sequential iterative algorithm [30]. These works try to minimize the number of interfering subnetworks, maximize the subnetworks achieving their target data rates, or minimize the interference-to-signal-ratios of the subnetworks given a limited amount of resources. However, subnetwork reconfigurations are not considered.

Summarizing, to the best of the authors' knowledge, guaranteeing interference-free operation while minimizing resource consumption and performing resource allocation to subnetworks also in the time domain, i.e., considering the reallocation of frequency resources based on future interference scenarios resulting in subnetwork reconfigurations, has not yet been investigated. Tackling these open challenges constitutes the motivation for the present work.

III. Problem Formulation

In this section, first, the general subnetwork system model and all parameters and symbols are introduced. Afterward, the optimization problem is mathematically formulated. All variables are listed in Table I in their order of appearance.

System Model and Frequency Subband Allocation: In this work, a set of mobile subnetworks $\mathcal{S}(t)$ connected to a single 6G umbrella network is considered during each time

TABLE I
LIST OF SYMBOLS

$\mathcal{S}(t)$	set of subnetws. in time step t	t	control var. for a time step
s	control var. for a subnetw.	a_s^{min}	min. freq. subband requirement of subnetw. s
$\mathcal{B}$	set of freq. subbands	$a_{s,b}(t)$	bin. var. for alloc. of freq. subband b to subnetw. s in time step t
$a_s(t)$	vector aggregating the vars. $a_{s,b}(t)$ for subnetw. s	$\boldsymbol{A}(t)$	freq. subband alloc. matrix for time step t
b	control var. for a freq. subband	t^n	current time step
t^f	number of time steps for which future positions are known	$\mathcal{T}$	set of time steps $\{t^n+1,...,t^n+t^f\}$
$i_{s,q}(t)$, $\boldsymbol{I}(t)$	var. indic. interference betw. subnetws. s and q in time step t, matrix summarizing the interference indicators $i_{s,q}(t)$	$b(t)$	number of used freq. subbands in time step t
$r(t,t-1)$	number of reconfigs. from time step $t-1$ to time step t	$f_1(t)$	first objective function, defined in (1a)
$f_2(t)$	second objective function, defined in (1b)	w_i	weighting factor for objective $f_i(t)$
c	control var. for a color	$\mathcal{C}$	set of colors used in the solution to a CGC problem
$\mathcal{S}_c(t)$	set of subnetws. colored with color c in time step t	$\gamma_s(t)$	var. indic. if subnetw. s' color changed from time step $t-1$ to t
$c_s(t)$	color of subnetw. s in time step t	n_p	number of graph permutations

step t (see Fig. 1). Every subnetwork s is associated with a constant frequency subband requirement a_s^{min} such that it can offer services to its users. The required subbands are allocated from the set of available frequency subbands $\mathcal{B}$ by the umbrella network. It is assumed that enough subbands are available to fulfill all subnetworks' demands at all times. Furthermore, it is assumed that the umbrella network and the subnetworks communicate via an out-of-band backhaul link. The allocation for a time step is summarized in the matrix $\boldsymbol{A}(t) \in \{0,1\}^{|\mathcal{S}(t)|\times|\mathcal{B}|}$ with elements $a_{s,b}(t)$, where $a_{s,b}(t)=1$ specifies that frequency subband b is allocated to subnetwork s at time step t, whereas $a_{s,b}(t)=0$ indicates that subband b cannot be used by subnetwork s at time step t.

Subnetwork Mobility and Interference: Since the subnetworks are considered to be mobile in this work, their position changes over time. It is assumed that the current position at $t=t^n$ as well as the future positions up to $t=t^n+t^f$ are known for every subnetwork. The future time instances for which the positions of all subnetwork APs are known are aggregated in the set $\mathcal{T}=\{t^n+1,...,t^n+t^f\}$. Based on these positions, it can be determined if two subnetworks s and q interfere with each other during a time step t in case they would use the same subbands. In case there would be interference, $i_{s,q}(t)=1$, and otherwise, $i_{s,q}(t)=0$. Due to the mobility of all subnetworks, the interference classification $i_{s,q}(t)$ also changes over time.[1] It is assumed that there is no intra-subnetwork interference due to orthogonal transmissions within each subnetwork.

Resource Usage and Subnetwork Reconfigurations: In total, $b(t)$ frequency subbands are used during a time step t. Since frequency spectrum is, in general, a limited resource, subbands should be reused in case two subnetworks do not interfere with each other. Thus, to ensure resource efficiency and interference-free operation for each subnetwork, the frequency subband allocation $\boldsymbol{A}(t)$ needs to be adjusted over time. However, the number of subnetwork reconfigurations, i.e., reallocations of subbands from one time step to another, denoted $r(t,t-1)$, should also be minimized to reduce the amount of signaling overhead both inside a subnetwork and from the umbrella network to the subnetworks. These two objectives are conflicting, which can be seen in the following example: Allocating single-use frequency subbands to all subnetworks would allow for no reconfigurations, however, the maximum amount of resources would be used.

[1]Note that the proposed optimization problem is agnostic to the method used to determine whether there is interference between two subnetworks.

Based on the known interference classification for $t\in\mathcal{T}$, the goal is to find these frequency subband allocations $\boldsymbol{A}(t)$ that, on the one hand, minimize the overall subband consumption, but, on the other hand, also minimize the number of reconfigurations. These objectives are mathematically formulated in the multi-objective optimization problem

$$\mathcal{P}_1\colon \min_{\boldsymbol{A}(t),t\in\mathcal{T}} \quad f_1(t)=\sum_{t\in\mathcal{T}} b(t), \tag{1a}$$

$$\min_{\boldsymbol{A}(t),t\in\mathcal{T}} \quad f_2(t)=\sum_{t\in\mathcal{T}} r(t,t-1) \tag{1b}$$

$$\text{s.t.} \quad \sum_{b\in\mathcal{B}} a_{s,b}(t)\geq a_s^{min}, \forall s\in\mathcal{S}(t), t\in\mathcal{T}, \tag{1c}$$

$$i_{s,q}(t)\cdot(a_{s,b}(t)+a_{q,b}(t))\leq 1, \quad \forall s,q\in\mathcal{S}(t), b\in\mathcal{B}, t\in\mathcal{T}, \tag{1d}$$

$$\prod_{b=j}^{j+a_s^{min}-1} a_{s,b}(t)=1, \forall s\in\mathcal{S}(t), t\in\mathcal{T}, \tag{1e}$$

$$a_{s,b}(t)\in\{0,1\}, \forall s\in\mathcal{S}(t), b\in\mathcal{B}, t\in\mathcal{T}, \tag{1f}$$

where j denotes the index of the first allocated subband.

In the problem formulation, the two objectives $f_1(t)$ and $f_2(t)$, defined by (1a) and (1b), are to minimize the sum over the used frequency subbands $b(t)$ and the sum of the subnetwork reconfigurations $r(t,t-1)$. The number $b(t)$ can be calculated by performing a logical OR operation over all rows of the allocation matrix $\boldsymbol{A}(t)$ and then summing over the resulting vector. The number of reconfigurations from one time step to another $r(t,t-1)$ is determined by checking whether the allocated subbands $a_s(t)$ for subnetwork s changed, i.e., a single reconfiguration is counted if $a_s(t)\neq a_s(t-1)$. This check is done for all $s\in\mathcal{S}(t)$. Constraint (1c) ensures that every subnetwork s is allocated enough subbands during every time step t to serve its users. In case two subnetworks would interfere with each other, they cannot use the same subband, which is captured by (1d). Constraint (1e) guarantees that all frequency subbands $\{j,...,j+a_s^{min}-1\}$ (at least a_s^{min} subbands) that are allocated to a single subnetwork s

during time step t are contiguous in the frequency domain.[2] Lastly, (1f) merely states that the decision variables are binary.

IV. Analysis and Solution Approaches

In the following, the optimization problem $\mathcal{P}_1$ is proven to be NP-hard, and its solution space is analyzed. Subsequently, different well-known multi-objective solution approaches are discussed. Finally, two heuristic algorithms developed specifically for the present optimization problem are proposed.

A. Optimization Problem Analysis

First, the NP-hardness of $\mathcal{P}_1$ is proven by proving the NP-hardness of a single-dimension version of $\mathcal{P}_1$ in Result 1.

Result 1. *Problem $\mathcal{P}_1$ is NP-hard.*

Proof. It is sufficient to show that the single-dimension optimization problem (1a) subject to constraints (1c)-(1f) is NP-hard since any multi-objective problem is NP-hard if any of its single-objective versions is NP-hard [31]. Assuming that the time step set $\mathcal{T}$ only consists of a single time step removes the time dimension of the problem. Furthermore, assuming that all $a_s^{min} = 1$ implies that constraint (1e) is fulfilled for any solution fulfilling the other constraints. The resulting optimization problem (1a) subject to constraints (1c), (1d), (1f) now reduces to a graph coloring problem, where every subnetwork s corresponds to a vertex and two vertices s and q are connected if $i_{s,q}(t) = 1$. Finding the chromatic number of this graph corresponds to minimizing the overall subband usage while guaranteeing that two interfering subnetworks do not use the same subband. Given that finding the chromatic number of a graph is NP-hard [32] concludes the proof. □

In general, multi-objective optimization problems consider multiple conflicting objective functions. For these kinds of optimization problems, there usually exists no single optimal solution, but rather multiple so-called Pareto optimal solutions [33]. A Pareto optimal solution is a solution where a single objective cannot be further improved unless another objective is degraded. In Fig. 2, the general "continuous" Pareto Frontier of $\mathcal{P}_1$ is depicted to visualize the dependency of the two objectives $f_1(t)$ and $f_2(t)$. On the one hand, it is discernible that it is possible to minimize the number of reconfigurations, i.e., $f_2(t)$, to 0. However, this comes at the cost of requiring $\sum_{t\in\mathcal{T}} a^{max}(t)$ subbands over the time steps $t \in \mathcal{T}$, where $a^{max}(t)$ depends on the actual interference scenario for these time steps. It can, however, be upper bounded by the sum of all subnetwork demands, i.e.,

$$a^{max}(t) \leq \sum_{s\in\mathcal{S}(t)} a_s^{min}.$$

On the other hand, it can be identified that the number of required subbands for $t \in \mathcal{T}$ can be minimized to $\sum_{t\in\mathcal{T}} a^{min}(t)$, where $a^{min}(t)$ again depends on the actual interference scenario, but can be lower bounded by the maximum required subbands of any subnetwork, i.e.,

$$\max_{s\in\mathcal{S}(t)} a_s^{min} \leq a^{min}(t).$$

Once more, there is a trade-off for this minimization of $f_1(t)$, which is the cost of $\sum_{t\in\mathcal{T}} r^{max}(t, t-1)$ reconfigurations over the time steps $t \in \mathcal{T}$. Thereby, $r^{max}(t, t-1)$ again depends on the actual interference scenario but can be upper bounded by the number of subnetworks that are present in both time step t and $t-1$, which can mathematically be expressed as

$$r^{max}(t, t-1) \leq \min\left(|\mathcal{S}(t)|, |\mathcal{S}(t-1)|\right).$$

Knowing the possible extreme objective values of optimization problem $\mathcal{P}_1$, the task is now to find a single or multiple Pareto optimal solutions along the Pareto Frontier. To this end, various solution approaches are discussed in the following subsection. In a real-world scenario, additionally, rules for choosing one of multiple Pareto optimal solutions need to be defined based on user preferences.

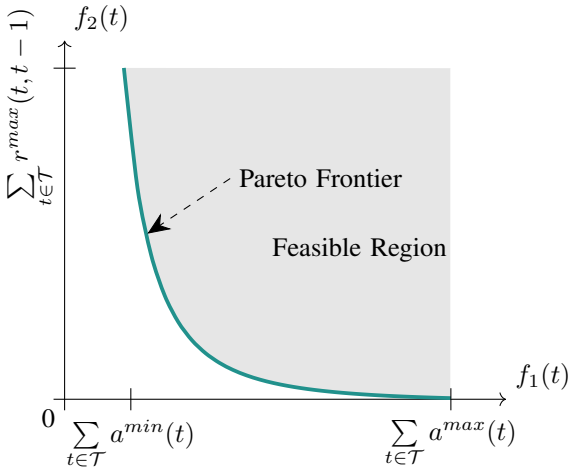

Fig. 2. The general "continuous" Pareto Frontier for optimization problem $\mathcal{P}_1$, where $r^{max}(t, t-1)$ denotes the worst case maximum number of reconfigurations from time step t to $t-1$, and $a^{min}(t)$ and $a^{max}(t)$ stand for the minimum possible number of used subbands allowing for interference-free operation or maximum required number of subbands allowing for no reconfigurations, respectively.

B. General Solution Approaches

The following introduces well-known solution approaches for multi-objective optimization that are employed for solving problem $\mathcal{P}_1$ during the simulations.

1) Scalarization

Scalarization is one of the most widely known methods for multi-objective optimization, which relies on converting the multi-objective optimization problem into a single-objective problem. This is achieved by associating every single objective $f_i(t)$ with a weight factor w_i and taking the weighted sum of the single objectives as the new objective [33]. Thus, scalarizing problem $\mathcal{P}_1$ leads to

$$\mathcal{P}_1^w\colon \min_{\boldsymbol{A}(t),t\in\mathcal{T}} \sum_{i=1}^{2} w_i f_i(t) \tag{2a}$$

$$\text{s.t.} \quad \text{(1c), (1d), (1e), (1f),} \tag{2b}$$

[2]Note that it is not necessary to include (1c) in the problem formulation during the optimization, as it is implicitly fulfilled in case (1e) is satisfied. Nevertheless, (1c) is kept in the formulation of $\mathcal{P}_1$ for clarity reasons.

with a single objective comprising the weighted sum of the two objectives $f_1(t)$ and $f_2(t)$. The great benefit of this method is that the solution found for $\mathcal{P}_1^w$ is guaranteed to be Pareto optimal if all $w_i > 0$ [33]. By choosing different weights for the single objectives, different Pareto optimal solutions can be found. Note that for non-convex problems, however, it is possible that some Pareto optimal solutions cannot be found no matter which weights are chosen. For a more detailed discussion of scalarization, the reader is referred to [33].

2) Lexicographic Ordering

Lexicographic ordering describes the process of prioritizing the single objectives of the multi-objective optimization problem according to the user's preferences. During the optimization of a lexicographic optimization problem, first, the most important objective is minimized. If the achieved solution is unique, the optimization process is stopped. Otherwise, the second-most important objective is minimized while not deteriorating the most important objective. This procedure is followed until a unique solution is found. Again, the solution to a lexicographic optimization problem is Pareto optimal. Hence, using this method allows for finding the extreme optimal solutions along the various objective directions. Note that in general, however, this method has the drawback of not allowing for a large improvement of a lower-prioritized objective at the cost of a small degradation of a higher-prioritized objective [33].

3) Unified Non-Dominated Sorting Genetic Algorithm-III

The Unified Non-Dominated Sorting Genetic Algorithm-III (U-NSGA-III) belongs to the class of evolutionary algorithms, which imitate natural evolution like crossover or mutation during the optimization process. Generally, advantages of evolutionary algorithms are Pareto Frontier coverage and solution diversity, while disadvantages are the bad ability to handle constraints and the demand for problem-specific parameter tuning [34]. U-NSGA-III was proposed in [35] as an enhancement to Non-Dominated Sorting Genetic Algorithm-III (NSGA-III) to improve handling bi-objective optimization problems [34]. In principle, U-NSGA-III searches solutions along reference directions specified in an M-dimensional space, where M denotes the number of objectives. The reference directions ideally cover the entire Pareto Frontier, allowing also the solutions to represent the shape of the Pareto Frontier. In contrast to scalarization and lexicographic ordering, the generated solution set from a single optimization run then provides the user with the possibility to select a single preferred solution. However, it must be noted that the solutions are not guaranteed to be optimal. For further information on evolutionary algorithms and U-NSGA-III, the reader is referred to [34], [35].

C. Heuristic Algorithms

Based on the knowledge that problem $\mathcal{P}_1$ can be reduced to a Centralized Graph Coloring (CGC) problem for certain cases, two heuristics relying on Greedy coloring the interference matrix were designed. To this end, the interference matrix is interpreted as an adjacency matrix of a graph, where two vertices are connected via an edge if the two corresponding subnetworks interfere with each other. The graph is then colored with the minimum possible number of colors, and all subnetworks with the same color are allocated the same subbands. Generally, for every graph coloring solution using colors c from the solution set $\mathcal{C}$, the total frequency subband demand is then determined as follows: First, find the maximum frequency subband demand a_s^{min} across all subnetworks s colored with the same color c. The subnetworks per color are grouped in the set $\mathcal{S}_c(t)$. Afterward, summing over these maximum values gives the total subband demand

$$b(t) = \sum_{c \in \mathcal{C}} \max_{s \in \mathcal{S}_c(t)} a_s^{min}. \tag{3}$$

Additionally, since it is assumed that the subband demand of a subnetwork does not change over time, the number of reconfigurations can simply be calculated by determining how many subnetworks were colored differently compared to the previous time step's coloring, i.e.,

$$r(t, t-1) = \sum_{s \in \mathcal{S}(t)} \gamma_s(t), \tag{4}$$

where $\gamma_s(t) = 1$ if the color of subnetwork s changed, i.e., $c_s(t-1) \neq c_s(t)$, and $\gamma_s(t) = 0$ otherwise. The following introduces the heuristic algorithms for finding the graph colorings for single time steps.

1) Greedy Minimizing Reconfigurations (GMR)

Greedily minimizing the reconfigurations of subnetworks only requires information about the interference scenario for the next upcoming time step as input. Jointly minimizing the reconfigurations and the resource usage can be done by taking over the coloring from time step $t-1$ and only adjusting these colors that are not assignable anymore due to new interference or that are not necessary anymore due to cleared interference. The heuristic works as follows: Starting with a single color, the number of available colors is increased until the graph coloring problem is solvable. The coloring is initialized with the solution from the previous time step if the color is available and still valid, i.e., no adjacent neighbor already has the same color. Then, the remaining vertices, i.e., subnetworks, are colored one by one. Once a solution is found, subnetworks with the same color are allocated the same subbands, and the subband usage and the number of reconfigurations can be calculated according to (3), (4). The procedure to find a coloring for the upcoming time step is summarized in Algorithm 1. Its computational complexity is $\mathcal{O}(n^4)$ since the while loop is run at most $|\mathcal{S}(t)|$ times and the color validity check (line 5 and 11) has complexity $\mathcal{O}(n)$. Thereby, n denotes the number of graph vertices, i.e., the number of present subnetworks $|\mathcal{S}(t)|$.

2) Permutation-Based Greedy Coloring (PBGC)

The PBGC is based on generating n_p graph permutations which are then colored using a Greedy coloring algorithm. Using the various colorings of the permuted interference matrices of single time steps, the best combination of these colorings can then be determined in terms of the subband demand and the number of reconfigurations by employing scalarization

Algorithm 1 Greedy Minimizing Reconfigurations (GMR)

Input: Interference matrix $\boldsymbol{I}(t)$
Output: Graph coloring $\boldsymbol{c}(t)$

1: Number of colors $n_c = 1$
2: **while** CGC problem not solvable **do**
3: $\quad \boldsymbol{c}(t) = -1$
4: $\quad$ **for** $s \in \mathcal{S}(t)$ **do**
5: $\quad\quad$ **if** $c_s(t-1) \leq n_c$ **and** $c_s(t-1)$ valid **then**
6: $\quad\quad\quad c_s(t) = c_s(t-1)$
7: $\quad$ **for** $s \in \mathcal{S}(t)$ **do**
8: $\quad\quad$ **if** $c_s(t) = -1$ **then**
9: $\quad\quad\quad c = 1$
10: $\quad\quad\quad$ **for** $c \leq n_c$ **do**
11: $\quad\quad\quad\quad$ **if** color c valid for subnetwork s **then**
12: $\quad\quad\quad\quad\quad c_s(t) = c$; break
13: $\quad\quad\quad\quad c = c + 1$
14: $\quad\quad\quad$ **if** $c_s(t) = -1$ **then**
15: $\quad\quad\quad\quad n_c = n_c + 1$; go to Line 3
16: $\quad$ **return** $\boldsymbol{c}(t)$

Algorithm 2 Permutation-Based Greedy Coloring (PBGC)

Input: Interference matrix $\boldsymbol{I}(t)\ \forall t \in \mathcal{T}$
Output: Graph coloring $\boldsymbol{c}(t^n + 1)$

1: **for** $t \in \mathcal{T}$ **do**
2: $\quad$ Greedily find min. number of colors for $\boldsymbol{I}(t)$
3: $\quad$ Generate n_p graph perm. and greedily color them
4: Generate all comb. of colorings for the time series $\mathcal{T}$
5: **for all** coloring combinations **do**
6: $\quad$ Calc. $f_1(t)$ acc. to (3), $f_2(t)$ acc. to (4)
7: Use scalarization or lexicographic ordering to find the best coloring combination, **return** $\boldsymbol{c}(t^n + 1)$

or lexicographic ordering. The pseudo-code for this solution approach is summarized in Algorithm 2. Its computational complexity is given as $\mathcal{O}(n_p^{t^f} \cdot t^f \cdot n)$, where n again denotes the number of graph vertices, i.e., $|\mathcal{S}(t)|$. The complexity is exponential in t^f, however, since t^f usually takes small values ($t^f \leq 5$), it can be interpreted as a constant, making the overall complexity of the proposed heuristic polynomial.

V. Performance Evaluation

In this section, first, the simulation setup and input data generation are described. Subsequently, a State-of-the-Art (SotA) benchmark based on CGC is introduced. Finally, the simulation results are presented and analyzed in detail.

A. Simulation Setup

To generate mobility data, vehicular movement based on the Manhattan Mobility Model [36] was simulated using the simulation framework SUMO [37]. The Manhattan grid was chosen to have a size of four vertices on the x-axis and three vertices on the y-axis, respectively. The vertices are equally spaced with an edge/street length of 50 m. Vehicle routes were generated randomly, and vehicles were generated with an arrival rate of 0.5 arrivals per second, which resulted in an average of 14.74 and a maximum of 20 present vehicles per time step. Based on the results from the vehicular movement simulation, which contain a position per vehicle per time step (second), the binary interference matrix was calculated. In case there exists a Line Of Sight (LOS) path between two vehicles, the Signal-to-Interference-plus-Noise Ratio (SINR) at a receiver spaced 2.5 m apart from its serving subnetwork AP was determined, which reflects a receiver positioned at the front or back of the vehicle. To this end, the received interference power from the second subnetwork was calculated using the LOS path loss formula for the Indoor Hotspot (InH) scenario defined in [38]. It is assumed that all subnetworks use the same transmission power. Based on the SINR, a binary decision for interference classification was taken. In case the SINR was larger than 10 dB, the considered two subnetworks do not interfere with each other. Otherwise, the two subnetworks were classified to be interfering, meaning that they cannot use the same frequency subbands. The threshold value 10 dB was chosen to allow for reliable communication with adequate throughput, i.e., to allow for a Channel Quality Indicator (CQI) value of 10, based on the mapping table from [39]. Using the described procedure, a binary interference matrix specifying whether two subnetworks interfere with each other during a single time step was determined for a total of 1050 time steps, ensuring sufficient randomness and variance for robust evaluation. The average number of interfering subnetworks is 2.65 per time step, while the maximum is 14. Lastly, to model the subband demand of each subnetwork, a random number was drawn from a discrete uniform distribution $\mathcal{U}\{1, 10\}$ upon the arrival of a vehicle in the network.

B. Benchmark: Centralized Graph Coloring (CGC)

To evaluate the performance of the proposed heuristic algorithms, similarly to the works [24]–[26], [28], [40], a benchmark based on CGC is used. To this end, the interference matrix $\boldsymbol{I}(t)$ is taken as the graph representation with vertices (subnetworks) connected via edges in case the subnetworks interfere with each other ($i_{s,q}(t) = 1$). For every time step t of the simulation, the graph coloring problem is optimally solved using backtracking. Afterward, the subband usage and the number of reconfigurations are calculated according to (3), (4). If multiple optimal graph coloring solutions achieve the same minimum subband usage, a single solution is randomly chosen from this set of solutions, disregarding the reconfigurations.

C. Simulation Results

First, to verify the theoretical Pareto Frontier introduced in Fig. 2, the optimization problem $\mathcal{P}_1$ was solved using lexicographic ordering and scalarization from Gurobi [41]. In total, $\mathcal{P}_1$ was solved for 1050 time steps for $t^f \in \{1, 2, 3\}$ using the interference matrices determined based on the mobility data as input.[3] Fig. 3 shows the averaged results from time steps 50 to 1050 in order to account for the warm-up phase

[3]Higher values of t^f prevented the employed solver from achieving optimal results within a reasonable timeframe.

of the vehicular movement simulation. Most importantly, it can be observed that better results are achieved the more information about future interference scenarios is available. Almost all depicted solutions for $t^f = 1$ are dominated by solutions for $t^f = 2$, which in turn are dominated by solutions for $t^f = 3$. It is important to note that results for the same scalarization weights for different t^f are not directly comparable to each other due to the higher influence of subband usage for higher t^f. Nevertheless, sweeping over all possible weights for $f_2(t)$ would result in all solutions with lower t^f being dominated by solutions with higher t^f.

Since the subband resource consumption can be minimized independently of t^f, the results for lexicographic ordering prioritizing the first objective $f_1(t)$ achieve the same minimum resource usage of 13.65 subbands. However, lower numbers of reconfigurations can be obtained for higher t^f. The improvement from $t^f = 1$ to $t^f = 3$ is 18.91 %.

As opposed to the theoretical minimum of zero reconfigurations shown in Fig. 2, this minimum cannot be seen in Fig. 3. The reason is that $\mathcal{P}_1$ is solved for every time step of the simulation. The average minimum achievable number of reconfigurations is larger than zero even when strictly prioritizing $f_2(t)$. The reason is that the current allocation $\boldsymbol{A}(t^n)$ is taken as input to calculate $r(t^n + 1, t^n)$ for the first upcoming time step, and, in some cases, it is not possible to find an allocation $\boldsymbol{A}(t^n + 1)$ that allows for zero reconfigurations. Again, the more information about future interference scenarios is available, the less is the average number of reconfigurations. For lexicographic ordering with priorities $(0, 1)$, the gain from $t^f = 1$ to $t^f = 3$ is 33.02 %, which, however, increases subband resource usage by 8.95 %.

Considering solutions found in the middle of the Pareto Frontier, e.g., scalarization with weights $(1, 2)$ for $t^f = 1$ and with weights $(1, 5)$ for $t^f = 3$, the improvement in terms of subband usage and reconfigurations is 2.77 % and 19.58 %.

Lastly, in the zoomed region of Fig. 3, it can be seen that the scalarization result for the weights $(1, 11)$ achieves a slightly lower number of reconfigurations than the results for the weights $(1, 15)$ and for lexicographic ordering prioritizing reconfigurations. Although this might seem irrational, the reason is again the current allocation $\boldsymbol{A}(t^n)$ that is taken as input to problem $\mathcal{P}_1$, which can result in allocations for earlier time steps that lead to later subband allocations allowing for a slightly smaller average number of reconfigurations.

Next, since, in general, scalarization and lexicographic ordering do not allow for a polynomial-time solution and only result in a single solution along the Pareto Frontier, U-NSGA-III [35], [42] was employed to solve problem $\mathcal{P}_1$. Reference directions were generated as equally spaced vectors between the extreme points of the Pareto Frontier. Although multiple parameter sets for the parameters *number of reference directions* and *population size* were investigated based on the reference numbers from [35] and the stopping criteria based on the objective value change were drastically relaxed [42], the algorithm did not find more than one solution for most of the time steps for any $t^f \in \{1, 2, 3\}$. This can be explained

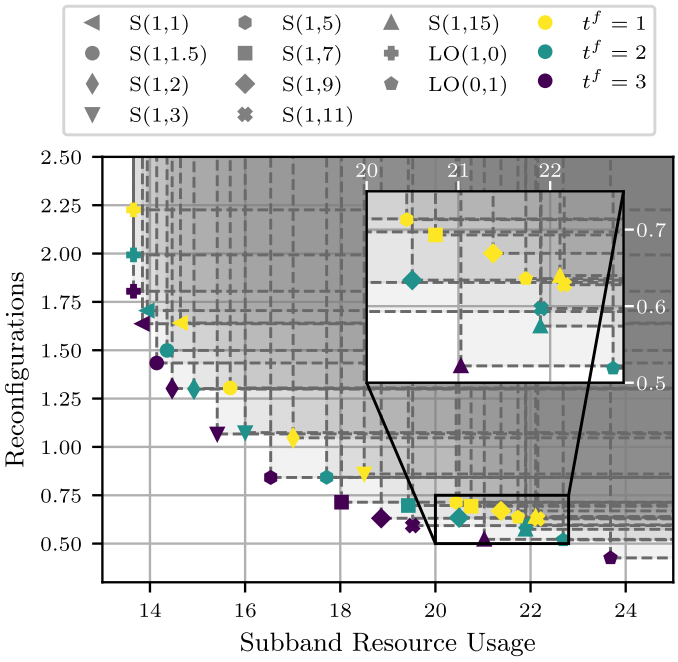

Fig. 3. Average results of 1000 time steps for scalarization (S) with the corresponding weights of the objective functions $f_1(t)$ and $f_2(t)$ $(w_{f_1(t)}, w_{f_2(t)})$ and for lexicographic ordering (LO) with the corresponding priorities of the objective functions $f_1(t)$ and $f_2(t)$ $(p_{f_1(t)}, p_{f_2(t)})$ for $t^f \in \{1, 2, 3\}$.

by the fact that the decision space that the U-NSGA-III explores is tremendously larger than the solution space of the optimization problem $\mathcal{P}_1$ due to the interference and contiguity constraints (1d) and (1e). Even though the algorithm converges to a feasible solution quite quickly, it only finds a solution that almost solely allocates single-use frequency subbands to the subnetworks. The average subband resource usage and reconfiguration results for $t^f \in \{1, 2, 3\}$ are summarized in Table II. The parameters were set as 20 reference directions and a population size of 200, and the termination tolerance was set to $5 \cdot 10^{-3}$, evaluated every 5^{th} generation for a window of 30 generations. For all other parameters, standard settings were chosen [42]. For every optimization run, the initial population was either randomly sampled or the final population from the previous time step was taken over as the initial population. Initializing the population with the previous final population allows for almost no reconfigurations since the vehicular mobility simulations start with a single subnetwork and thus allow the U-NSGA-III to find an optimal solution for the first few time steps from where it can evolve. Moreover, the number of reconfigurations slightly decreases for higher t^f, however, the subband usage increases. For randomly initialized populations, the U-NSGA-III is not able to use the information about future interference scenarios and achieves bad results overall. These results show that the U-NSGA-III is not able to sufficiently explore the solution space and adequately exploit the information about future interference scenarios.

Finally, the performance of the heuristic algorithms GMR and PBGC is evaluated. Simulation results for various numbers of graph permutations n_p are depicted in Fig. 4. Note that in all three subplots, the data point for GMR is the same, as

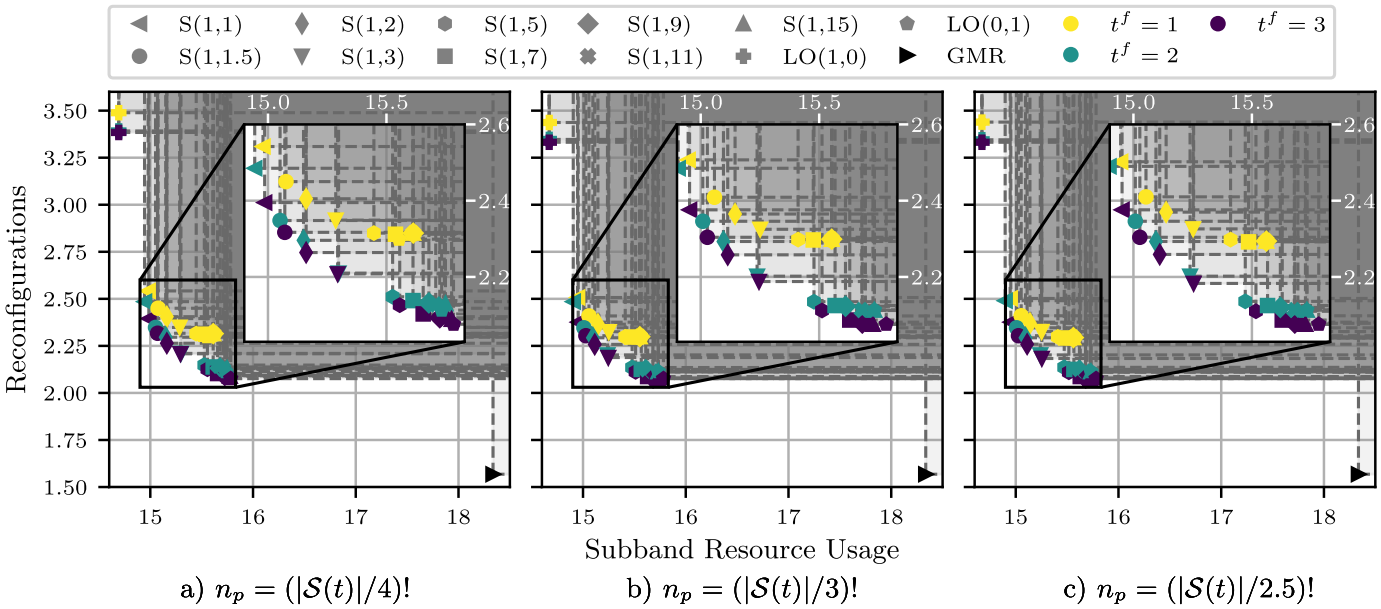

Fig. 4. Average results of 1000 time steps for GMR and PBGC using scalarization (S) with weights $(w_{f_1(t)}, w_{f_2(t)})$ and lexicographic ordering (LO) with priorities $(p_{f_1(t)}, p_{f_2(t)})$ for $t^f \in \{1, 2, 3\}$ for different n_p.

TABLE II
RESOURCE USAGE AND RECONFIGURATIONS FOR $t^f \in \{1, 2, 3\}$ ACHIEVED WITH U-NSGA-III

Init. Pop. \ t^f		1	2	3
Rand. Sampling	Subband Res. Usage	45.73	46.40	46.76
	Reconfig.	7.85	10.99	11.81
Prev. Fin. Pop.	Subband Res. Usage	39.55	44.51	44.09
	Reconfig.	0.37	0.36	0.29

the heuristic does not depend on n_p. It can be observed that, despite its simplicity, the GMR heuristic performs very well compared to the Pareto optimal results. It achieves an average subband resource usage of 18.34 while only requiring an average of 1.57 subnetwork reconfigurations. For a similar subband usage, the minimum achievable number of reconfigurations for $t^f = 1$ is 0.86, obtained with scalarization weights $(1, 3)$.

Examining the PBGC heuristic, even for a small n_p, see Fig. 4a), the minimum achieved subband usage is 14.69, which is only 7.61 % worse than the optimal value achieved with lexicographic ordering. Note that it is impossible to achieve the Pareto optimal results depicted in Fig. 3, as solving $\mathcal{P}_1$ using CGC and afterward allocating the number of subbands according to the maximum demand of a subnetwork from the set $\mathcal{S}_c(t)$ is a simplification of the original optimization problem. This can also be seen when comparing the lexicographic ordering results of PBGC against the optimal CGC coloring, which achieves an average subband resource usage of 14.68.

In general, it must be noted that the average number of reconfigurations lies between 1.5 and 3.5 for all numbers of graph permutations n_p, which is, on average, twice as high as the optimal results. The reason is that applying Greedy coloring to various graph permutations still only provides a small subset of possible solutions. Nevertheless, better results are achieved the larger the number of permutations n_p is.

Lastly, even though the number of reconfigurations achieved with the PBGC heuristic is generally higher, the algorithm is capable of exploiting the information about future interference scenarios. Solutions for $t^f = 1$ are again dominated by solutions for $t^f = 2$, and in turn are dominated by solutions for $t^f = 3$. Looking at the results from Fig. 4c) for scalarization with weights $(1, 3)$ for $t^f = 1$ and with weights $(1, 2)$ for $t^f = 3$, the improvement in terms of subband usage and reconfigurations is 0.93 % and 2.88 %. This validates the approach of considering multiple time steps for frequency resource allocation to subnetworks in order to minimize the overall resource consumption and subnetwork reconfigurations while guaranteeing interference-free operation of all subnetworks.

VI. CONCLUSION

In this paper, an optimization problem for centralized frequency subband allocation to mobile 6G in-X subnetworks in the coverage area of an umbrella network was formulated. The novel approach of considering movement trajectories of the vehicles carrying the subnetwork APs allows for safely predicting future interference scenarios, which enables the joint minimization of subband usage and subnetwork reconfigurations. Employing various multi-objective optimization solution methods and two heuristic algorithms called GMR and PBGC in a realistic simulation, the value of the knowledge about future interference scenarios was highlighted. Specifically, depending on the optimization goal, the reconfigurations can be reduced by 18.91 % when primarily minimizing subband usage, by 19.58 % while reducing subband usage by 2.77 %, and even by 33.02 % when primarily minimizing reconfigurations, if the interference scenarios are known for the upcoming three time steps instead of only a single time step. When using the PBGC heuristic, reconfigurations can still be reduced by 2.88 % while reducing the subband usage by 0.93 %. Developing a heuristic or employing ML for distributed channel selection considering knowledge about future interference scenarios is seen as possible future work.

REFERENCES

[1] S. Wang and C. Ran, "Rethinking cellular network planning and optimization," *IEEE Wirel. Commun.*, vol. 23, no. 2, 2016.

[2] J. Cheung, M. Beach, and J. McGeehan, "Network planning for third-generation mobile radio systems," *IEEE Commun. Mag.*, vol. 32, no. 11, 1994.

[3] K. Tutschku, "Demand-based radio network planning of cellular mobile communication systems," in *Proc. IEEE INFOCOM*, vol. 3, 1998.

[4] S.-E. Elayoubi, O. Ben Haddada, and B. Fourestie, "Performance evaluation of frequency planning schemes in OFDMA-based networks," *IEEE Trans. Wirel. Commun.*, vol. 7, no. 5, 2008.

[5] H. Viswanathan and P. E. Mogensen, "Communications in the 6G era," *IEEE Access*, vol. 8, 2020.

[6] B. Kim, D. Calin, N. Tenny, M. Shariat, and M. Fan, "Device centric distributed compute, orchestration and networking," *IEEE Wirel. Commun.*, vol. 30, no. 4, 2023.

[7] M. Hoffmann, G. Kunzmann, T. Dudda, R. Irmer, A. Jukan, G. Macher, A. Ahmad, F. R. Beenen, A. Bröring, F. Fellhauer, G. P. Fettweis, F. H. P. Fitzek, N. Franchi, F. Gast, B. Haberland, S. Hoppe, S. Joodaki, N. P. Kuruvatti, C. Li, M. Lopez, F. Mehmeti, T. Meyerhoff, L. Miretti, G. T. Nguyen, M. Parvini, R. Pries, R. F. Schaefer, P. Schneider, D. A. Schupke, S. Strassner, H. Stubbe, and A. M. Voicu, "A secure and resilient 6G architecture vision of the german flagship project 6G-ANNA," *IEEE Access*, vol. 11, 2023.

[8] M. A. Uusitalo, P. Rugeland, M. R. Boldi, E. C. Strinati, P. Demestichas, M. Ericson, G. P. Fettweis, M. C. Filippou, A. Gati, M.-H. Hamon, M. Hoffmann, M. Latva-Aho, A. Pärssinen, B. Richerzhagen, H. Schotten, T. Svensson, G. Wikström, H. Wymeersch, V. Ziegler, and Y. Zou, "6G vision, value, use cases and technologies from european 6G flagship project Hexa-X," *IEEE Access*, vol. 9, 2021.

[9] V. Ziegler, H. Viswanathan, H. Flinck, M. Hoffmann, V. Räisänen, and K. Hätönen, "6G architecture to connect the worlds," *IEEE Access*, vol. 8, 2020.

[10] G. Berardinelli, P. Mogensen, and R. O. Adeogun, "6G subnetworks for life-critical communication," in *2020 2nd 6G Wireless Summit (6G SUMMIT)*, 2020.

[11] X. Du, T. Wang, Q. Feng, C. Ye, T. Tao, L. Wang, Y. Shi, and M. Chen, "Multi-agent reinforcement learning for dynamic resource management in 6G in-X subnetworks," *IEEE Transactions on Wireless Communications*, vol. 22, no. 3, 2023.

[12] Y. Hu, M. C. Gursoy, and A. Schmeink, "Relaying-enabled ultra-reliable low-latency communications in 5G," *IEEE Netw.*, vol. 32, no. 2, 2018.

[13] M. Wen, Q. Li, K. J. Kim, D. López-Pérez, O. A. Dobre, H. V. Poor, P. Popovski, and T. A. Tsiftsis, "Private 5G networks: Concepts, architectures, and research landscape," *IEEE J. Sel. Top. Signal Process.*, vol. 16, no. 1, 2022.

[14] G. Berardinelli, P. Baracca, R. O. Adeogun, S. R. Khosravirad, F. Schaich, K. Upadhya, D. Li, T. Tao, H. Viswanathan, and P. Mogensen, "Extreme communication in 6G: Vision and challenges for 'in-X' subnetworks," *IEEE Open J. Commun. Soc*, 2021.

[15] R. Adeogun, "Federated deep deterministic policy gradient for power control in 6G in-X subnetworks," in *Proc. IEEE ICEENG*, 2024.

[16] D. Abode, R. Adeogun, and G. Berardinelli, "Power control for 6G industrial wireless subnetworks: A graph neural network approach," in *Proc. IEEE WCNC*, 2023.

[17] D. Abode, R. Adeogun, and G. Berardinelli, "Power control for 6G in-factory subnetworks with partial channel information using graph neural networks," *IEEE Open J. Commun. Soc.*, vol. 5, 2024.

[18] D. Abode, G. Berardinelli, R. Adeogun, P. Maia de Sant Ana, and A. Artemenko, "Control-aware transmit power allocation for 6G in-factory subnetwork control systems," in *Proc. IEEE GLOBECOM*, 2024.

[19] D. Li, S. R. Khosravirad, T. Tao, P. Baracca, and P. Wen, "Power allocation for 6G sub-networks in industrial wireless control," in *Proc. IEEE WCNC*, 2024.

[20] M. Elwekeil, L. G. Giordano, P. Baracca, and S. Buzzi, "Distributed MIMO for 6G sub-networks in the unlicensed spectrum," in *Proc. IEEE CSCN*, 2023.

[21] R. Adeogun and G. Berardinelli, "Distributed channel allocation for mobile 6G subnetworks via multi-agent deep Q-learning," in *Proc. IEEE WCNC*, 2023.

[22] A. Srinivasan, U. Singh, and O. Tirkkonen, "Multi-agent reinforcement learning approach scheduling for in-X subnetworks," in *Proc. IEEE VTC Fall*, 2024.

[23] R. Adeogun and G. Berardinelli, "Multi-agent dynamic resource allocation in 6G in-X subnetworks with limited sensing information," *Sensors*, vol. 22, no. 13, 2022.

[24] B. Madsen and R. Adeogun, "Federated multi-agent DRL for radio resource management in industrial 6G in-X subnetworks," in *Proc. IEEE PIMRC*, 2024.

[25] R. Adeogun, G. Berardinelli, I. Rodriguez, and P. Mogensen, "Distributed dynamic channel allocation in 6G in-X subnetworks for industrial automation," in *IEEE GC Wkshps*, 2020.

[26] R. Adeogun, G. Berardinelli, and P. Mogensen, "Learning to dynamically allocate radio resources in mobile 6G in-X subnetworks," in *Proc. IEEE PIMRC*, 2021.

[27] S. Bagherinejad, T. Jacobsen, N. Kiilerich Pratas, and R. Adeogun, "Comparative analysis of sub-band allocation algorithms in in-body subnetworks supporting XR applications," in *Proc. IEEE WCNC*, 2024.

[28] D. Abode, G. Berardinelli, R. Adeogun, L. Salaun, R. Abreu, and T. Jacobsen, "Unsupervised graph-based learning method for sub-band allocation in 6G subnetworks," in *Proc. IEEE VTC Fall*, 2024.

[29] S. Hakimi, R. Adeogun, and G. Berardinelli, "Rate-conforming sub-band allocation for in-factory subnetworks: A deep neural network approach," in *Proc. IEEE EuCNC/6G Summit*, 2024.

[30] D. Li, S. R. Khosravirad, T. Tao, and P. Baracca, "Advanced frequency resource allocation for industrial wireless control in 6G subnetworks," in *Proc. IEEE WCNC*, 2023.

[31] F. Bökler, "The multiobjective shortest path problem is NP-hard, or is it?," in *Evolutionary Multi-Criterion Optimization*, Springer International Publishing, 2017.

[32] M. R. Garey and D. S. Johnson, *Computers and Intractability: A Guide to the Theory of NP-Completeness (Series of Books in the Mathematical Sciences)*. W. H. Freeman and Company, San Francisco, 1979.

[33] J. Branke, K. Deb, K. Miettinen, and R. Slowinski, eds., *Multiobjective Optimization, Interactive and Evolutionary Approaches [outcome of Dagstuhl seminars]*, vol. 5252 of *Lecture Notes in Computer Science*, Springer, 2008.

[34] S. Sharma and V. Kumar, "A comprehensive review on multi-objective optimization techniques: Past, present and future," *Arch. Computat. Methods Eng.*, vol. 29, no. 7, 2022.

[35] H. Seada and K. Deb, "A unified evolutionary optimization procedure for single, multiple, and many objectives," *IEEE Trans. Evol. Comput.*, vol. 20, no. 3, 2016.

[36] S. Gowrishankar, S. Sarkar, and T. Basavaraju, "Simulation based performance comparison of community model, GFMM, RPGM, Manhattan model and RWP-SS mobility models in MANET," in *Proc. IEEE NETCOM*, 2009.

[37] P. A. Lopez, M. Behrisch, L. Bieker-Walz, J. Erdmann, Y.-P. Flötteröd, R. Hilbrich, L. Lücken, J. Rummel, P. Wagner, and E. Wießner, "Microscopic traffic simulation using SUMO," in *Proc. IEEE ITSC*, 2018.

[38] ETSI, "5G study on channel model for frequencies from 0.5 to 100 GHz: 3GPP TR 38.901 version 18.0.0 release 18." www.etsi.org, 2024. Technical Requirement.

[39] OpenAirInterface Software Alliance, "OpenAirInterface (OAI) PHY Code: NR_UE_TRANSPORT/csi_rx.c." https://gitlab.eurecom.fr/oai/openairinterface5g/-/blob/develop/openair1/PHY/NR_UE_TRANSPORT/csi_rx.c. Accessed: 2024-09-09.

[40] G. Berardinelli and R. Adeogun, "Hybrid radio resource management for 6G subnetwork crowds," *IEEE Commun. Mag.*, vol. 61, no. 6, 2023.

[41] Gurobi Optimization, LLC, "Gurobi Optimizer Reference Manual," 2024.

[42] J. Blank and K. Deb, "pymoo: Multi-objective optimization in python," *IEEE Access*, vol. 8, 2020.